Phys Chem Minerals (2012) 39:213–218
DOI 10.1007/s00269-011-0476-6

ORIGINAL PAPER

Grain growth kinetics and the effect of crystallographic anisotropy on normal grain growth of quartz

Katsuyoshi Michibayashi · Hisashi Imoto

Received: 8 August 2011 / Accepted: 14 December 2011 / Published online: 30 December 2011

Abstract Annealing experiments on agate were performed to investigate grain growth kinetics and the effect of crystallographic anisotropy on normal grain growth of quartz. The experiments were conducted using a piston-cylinder apparatus at 700–800°C and 0.5 GPa for 0–66 h. The grain growth rate was expressed by $D^n - D_0^n = kt$ with $k = k_0 \exp(-H^*/RT)$ where D_0 is the initial grain size at $t = 0$, with $n = 4.4 \pm 0.3$, and $H^* = 191.3 \pm 11.0$ kJ/mol is the activation enthalpy and $\log k_0 = 19.8 \pm 1.4$. While the grain aspect ratios are nearly constant at ~ 0.7 (short/long) during grain growth, the longest axis in individual grains tends to be oriented parallel to their *c*-axis, indicating that a primary crystal-preferred orientation of *c*-axis of the agate could result in the development of a weak shape-preferred orientation during grain growth.

Keywords Quartz · Normal grain growth kinetics · Crystal-preferred orientation · Shape-preferred orientation · Grain size · Grain shape

Introduction

The grain size of rocks is an important parameter in understanding the dynamics of the Earth's interior (e.g., Austin and Evans 2007; Karato 2008). Static grain growth is a relatively simple transformation in which grain size increases under driving forces related to the curvature of grain and interphase boundaries (e.g., Atkinson 1988; Yamazaki et al. 2005; Ohuchi and Nakamura 2007). However, there are few quantitative studies on grain growth of quartz (e.g., Tullis and Yund 1982; Karato 2008). Furthermore, until recently, it was difficult to measure the size, shape, and crystallographic orientation of each grain precisely, although this is now possible with the development of the electron back-scattered diffraction technique (EBSD) by scanning electron microscope (SEM). Even in closely controlled laboratory experiments, growth kinetics may be complicated and unconstrained; consequently, additional data are needed to accurately predict growth rates in nature (Evans et al. 2001; Karato 2008).

In this paper, we present the results of experiments on the static grain growth of a quartz aggregate in a solid confining medium high-pressure/high-temperature apparatus. We chose agate as a starting material because it consists of very fine-grained quartz aggregates with an intense crystal-preferred orientation (CPO) of *c*-axis, with the result that we found an effect of crystallographic anisotropy on the normal grain growth of quartz. These results were partly presented by Imoto and Michibayashi (2010); however, because this earlier paper is written in Japanese and was not subjected to peer-review, we combine their results with the rest of our experimental data in this paper.

Experimental procedure

Starting material

The starting material is agate, which is natural pure quartzite with an average grain size of <1 μm. The agate sample contains approximately 1.5 weight percent water (Watanabe 2007) and has a characteristic fibrous texture (e.g., Masuda et al. 1997). The *c*-axis [001] of the agate defines a girdle pattern in a stereonet, perpendicular to the

K. Michibayashi (✉) · H. Imoto
Institute of Geosciences, Shizuoka University,
Shizuoka 422-8529, Japan
e-mail: sekmich@ipc.shizuoka.ac.jp

orientation of the fibrous texture (Imoto and Michibayashi 2010). For the annealing experiment, the agate was cored and sliced to prepare cylindrical samples of 22 mm long and 10 mm in diameter.

Specimen assembly and apparatus

Annealing experiments were performed using a Griggs-type piston-cylinder apparatus, MK65S (e.g., Masuda and Fujimura 1981; Masuda et al. 1997; Shimizu et al. 2006), which was constructed at Shizuoka University, Japan, and has a maximum confining pressure of 1.5 GPa and a maximum temperature of 1,200°C. The apparatus is able to measure confining pressure more precisely than a conventional Griggs-type solid deformation apparatus (Shimizu et al. 2006).

Figure 1 shows the assembly used for the annealing experiments. The sample was heated by a graphite tube heater and was surrounded by a pyrophyllite confining-pressure medium. The specimen was surrounded by a thin pyrophyllite sleeve to avoid direct contact with the heater. Confining pressure was applied to the specimen by compressing the pressure medium axially, using two outer pistons. The temperature was monitored by K-type thermocouples on the central surfaces of the specimen. In this setup, the difference in temperature between the top and central surfaces is about 40 and 50°C in the case of central surface temperatures of 800 and 1,000°C, respectively (Masuda and Fujimura 1981). Confining pressure was measured by load cells located at the outer piston. Logs of temperature and confining pressure were recorded on a personal computer using LabVIEW (National Instruments Corporation).

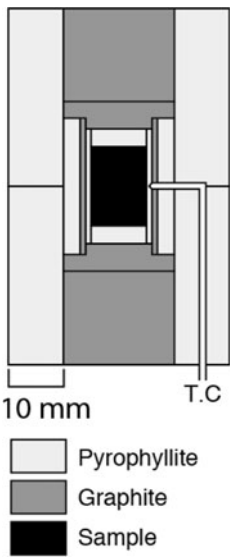

Fig. 1 Schematic of the specimen assembly used in the experiments. T.C.: thermocouple

Annealing conditions

The experiments were conducted at temperatures of 700 and 800°C, a confining pressure of 0.5 GPa, and annealing times of 0–66 h (Table 1). During each experiment, the confining pressure was first increased to about 80% of the desired pressure for several hours. The temperature was slowly increased to 600°C over the next few hours and maintained at this level for 1 h. This was done because pyrophyllite releases water under these conditions. With increasing temperature, the confining pressure was increased up to tens of MPa. The confining pressure and temperature were then simultaneously increased to the required levels. After the experiment, the confining pressure was slowly reduced to room pressure over about 24 h and the temperature was rapidly dropped to room temperature over several minutes.

Analytical method

All of the annealed samples were cut parallel to the long axis. One half of each annealed sample was impregnated with resin prior to preparing polished thin sections or thick sections for microstructural analyses.

Grain boundaries at the center of each annealed sample were carefully traced from a secondary electron image of the sample microstructure taken using a scanning electron microscope (JEOL JSM6300) housed at the Center for Instrumental Analysis, Shizuoka University, Japan. The grain sizes (D) of all samples were measured using Scion image analyse software. The grain size of each grain is represented by the diameter of a circle with an equivalent area to that of the grain (e.g., Michibayashi and Masuda 1993; Masuda et al. 1997).

The samples annealed at 800°C show clear microstructures; consequently, we measured the shape parameters (aspect ratio L (short/long axis)) and the orientation of the long axis (ϕ) of quartz grains, as well as their grain sizes.

Crystal-preferred orientations (CPO) of quartz were measured from highly polished thin sections using a JEOL 6300 SEM equipped with electron back-scattered diffraction (EBSD) at Shizuoka University (e.g., Michibayashi et al. 2007, 2009; Katayama et al. 2009; Muramoto et al. 2011). We determined between 198 and 201 quartz crystal orientations per sample and visually checked the computerized indexation of the diffraction pattern for each crystal orientation.

Results

The annealed samples consist of granular and polygonal quartz grains without undulose extinctions (Fig. 2). The

grain size distributions are log-normal (Fig. 3), and the mean grain size, D [μm], calculated using a log scale, increases with increasing annealing time, t [s], as shown in Fig. 4. The relationship between D and t for the experiments is expressed by $D = Kt^{0.184 \pm 0.005}$, where K is a temperature-dependent rate constant (Fig. 4).

Table 1 Experimental conditions and grain size data

Sample no.	Material	Temperature (°C)	Pressure (GPa)	Time (h)	Logarithmic mean grain size log(μm)	Standard deviation log(μm)	Standard error log(μm)	Mean grain size (μm)
IMO-005*	Agate	800	0.5	0.5	0.43	0.15	0.006	2.69
IMO-007*	Agate	800	0.5	24	0.64	0.20	0.019	4.37
IMO-008*	Agate	800	0.5	66	0.90	0.35	0.024	7.94
IMO-011	Agate	700	0.5	6	0.12	0.21	0.074	1.32
IMO-012	Agate	700	0.5	31	0.28	0.22	0.023	1.91

* Data from Imoto and Michibayashi (2010)

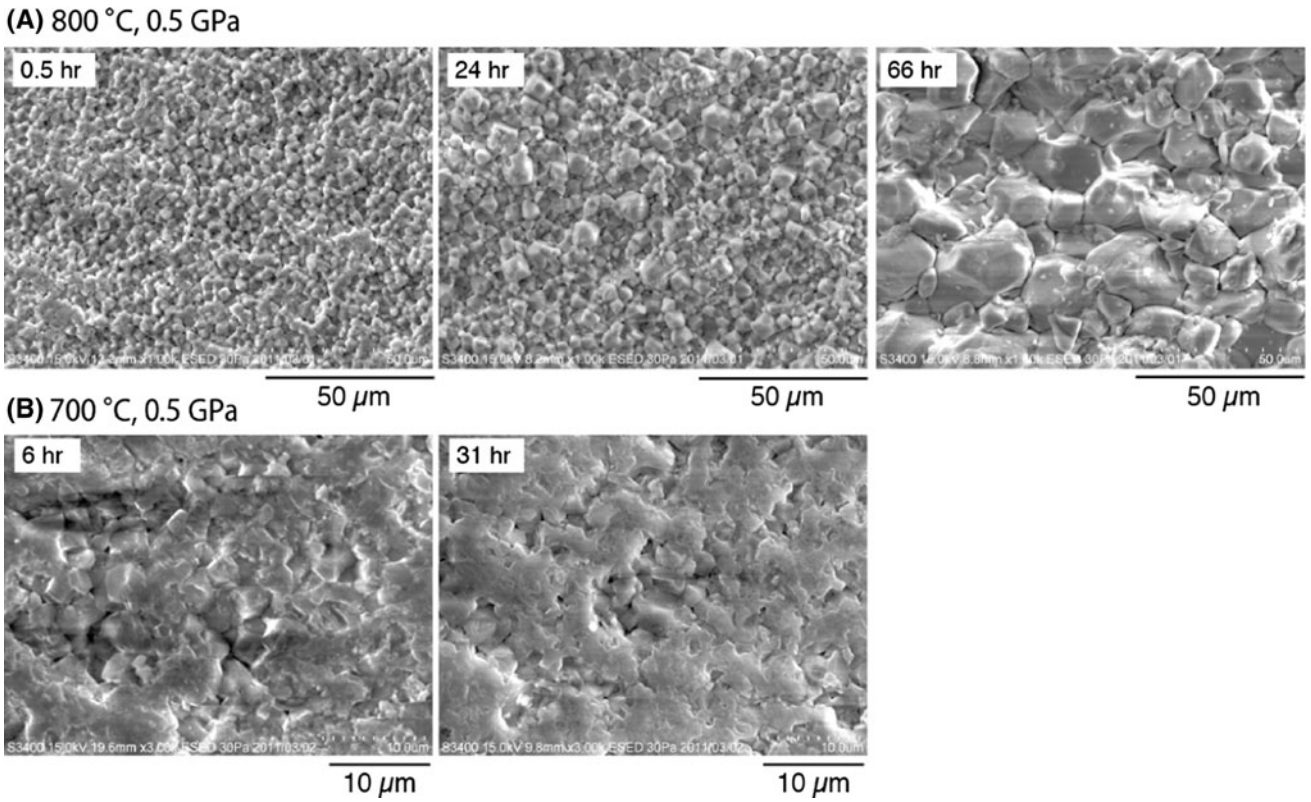

Fig. 2 Secondary electron images of quartz aggregates in annealed samples (Hitachi S-3400N Type II, Shizuoka University)

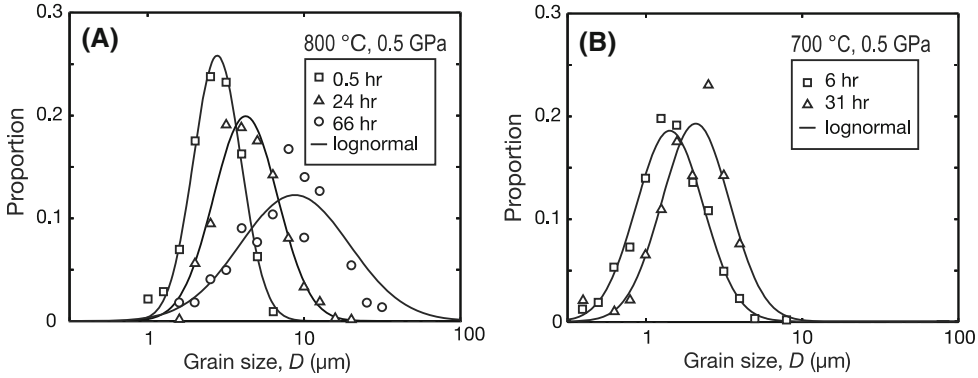

Fig. 3 Grain size distributions of quartz aggregates in annealed agates

The aspect ratios for the samples annealed at 800°C show a normal distribution (Fig. 5a–b); however, the mean aspect ratio, L_{mean}, is similar for all samples, in contrast to grain size (compare Figs. 3, 5a–b). Whereas the mean aspect ratios are ~0.7, the orientation distributions show that shape-preferred orientations are more intense with increasing grain size (Fig. 5c–d). Quartz CPOs are defined by a girdle of *c*-axis oriented parallel to a great circle, representing the primary CPO of the agate (Fig. 5e–f).

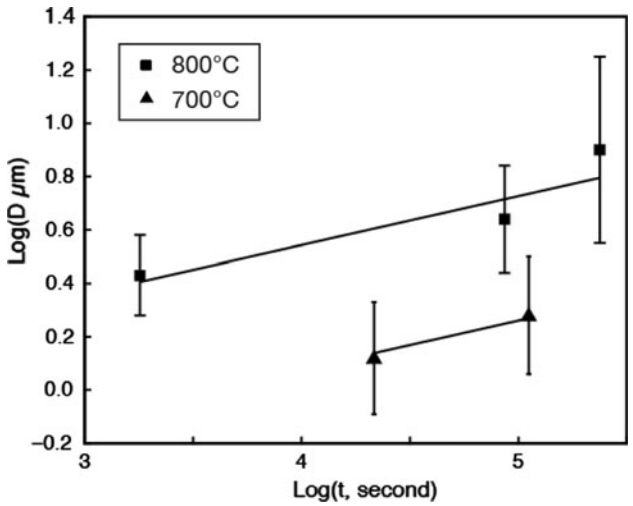

Fig. 4 Mean grain sizes of quartz aggregates in annealed agates with respect to annealing time. The *solid lines* represent grain growth trends according to $D = Kt^{0.184 \pm 0.005}$

Discussion

Several features are common to all of the annealed samples: grains are polygonal, grain diameters show a log-normal distribution (Fig. 3), the mean grain diameter increases with increasing annealing time (Fig. 4), and the largest grain in each experiment is less than five times the mean grain diameter. These findings indicate the occurrence of normal grain growth (e.g., Ohuchi and Nakamura 2007).

Grain growth kinetics

Normal grain growth over time is commonly described as follows:

$$D^n - D_0^n = kt, \quad (1)$$

where $k = k_0 \exp(-H^*/RT)$, D is the grain size after annealing time t, D_0 is the hypothetical initial grain size, n is a grain growth exponent, k_0 is a pre-exponential constant, H^* is activation enthalpy, R is the molar gas constant, and T is temperature. We determined n, D_0, and k in the Eq. (1) by a non-linear least squares method and subsequently H^* and k_0 were calculated on an Arrhenius plot (Fig. 6). As a result, we obtained $n = 4.4 \pm 0.3$, $D_0 = 0.54 \pm 0.44$, $H^* = 191.3 \pm 11.0$ kJ/mol, and $\log k_0 = 19.8 \pm 1.4$.

The grain growth exponent n is considered to be a geometric factor and depends on the rate-limiting processes

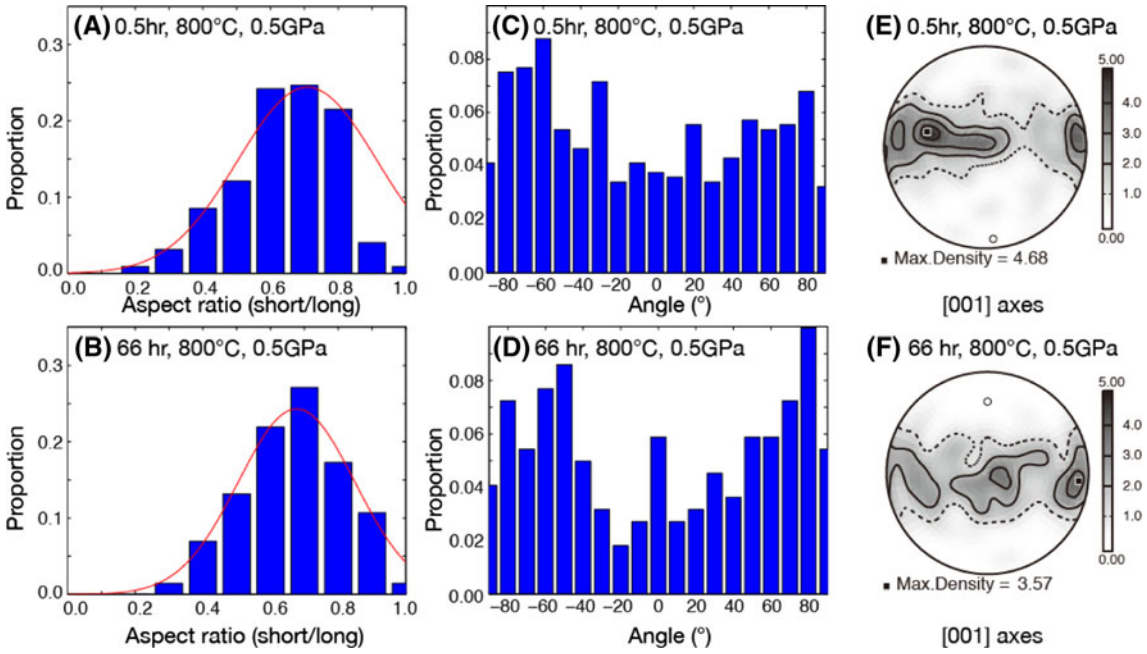

Fig. 5 **a** and **b** Aspect ratios of quartz aggregates in annealed agate samples after 0.5 and 66 h, respectively. Best-fit curves are shown for a log-normal distribution. **c** and **d** Orientation distributions of the long axis of quartz grains with respect to a horizontal reference line for individual grains within the quartz aggregates in the annealed agate samples after 0.5 and 66 h, respectively. **e** and **f** Orientations of quartz [001] axis within quartz aggregates in annealed agate samples after 0.5 and 66 h, respectively

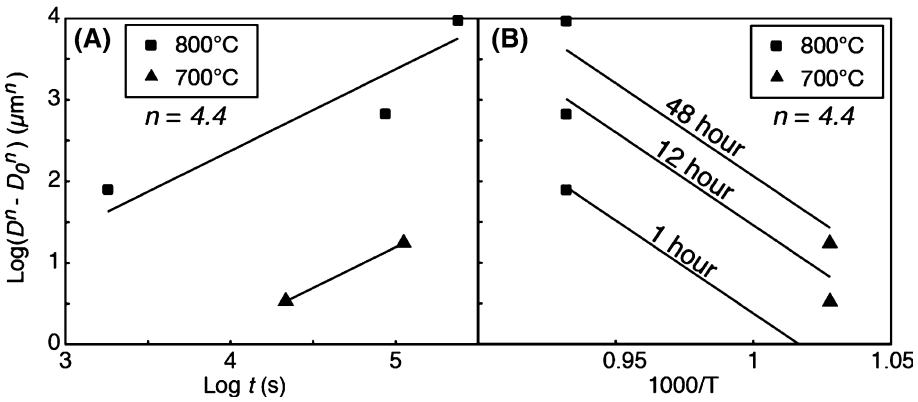

Fig. 6 Grain growth rate of quartz aggregates in annealed agates at the pressure of 0.5 GPa. **a** As a function of annealing time at temperatures of 700 and 800°C. **b** As a function of reciprocal temperature for different annealing times. *Solid lines* indicate the non-linear least square fit to the grain growth law: $D^n - D_0^n = k_0 \exp(-H^*/RT)t$, yielding $n = 4.4 \pm 0.3$, $H^* = 191.3 \pm 11.0$ kJ/mol, $\log k_0 = 19.8 \pm 1.4$, and $D_0 = 0.54 \pm 0.44$

of the grain growth (Evans et al. 2001). The theoretical values of n are generally in the range of 1–5, most of which are calculated for single and quasi-single polycrystallines (Atkinson 1988; Yamazaki et al. 2005; Ohuchi and Nakamura 2007). Karato (2008) recalculated grain growth parameters of quartz based on the experiments by Tullis and Yund (1982) and obtained $n \sim 2$, $H^* = 80$ kJ/mol, and $\log k_0 = 2$, which is smaller than the present result.

The starting material was different between this study (agate) and Tullis and Yund (1982), who used novaculite and flint. Tullis and Yund (1982) proposed that grain growth kinetics is controlled by the solubility of quartz in the interstitial fluid. Our preliminary result, also based on experiments using the MK65S apparatus, showed that the grain growth rate of quartz in flint is much faster than that in agate (Ueta and Michibayashi 2010). Karato (2008) pointed out that grain growth kinetics is further sensitive to other parameters such as oxygen fugacity and water content. Therefore, it seems that the difference in the starting material between the present study and Tullis and Yund (1982) could result in a rather contrasting grain growth rate of quartz.

The effect of crystallographic anisotropy

Our experimental results show that while the grain size of quartz increased from a few microns to a few tens of microns with time, grain shape was nearly constant, becoming slightly elongated (Figs 4, 5a–b). However, the orientation distributions of the longest axis in such slightly elongate grains are anisotropic, even for an annealing time of 0.5 h (Fig. 5c–d). Furthermore, the orientations of grain long axis tend to be parallel to their *c*-axis (Figs. 5, 7). Kruhl (2001) showed that during normal grain growth, the crystallographic orientation affects not only the shape and orientation of grain boundaries, but also the development

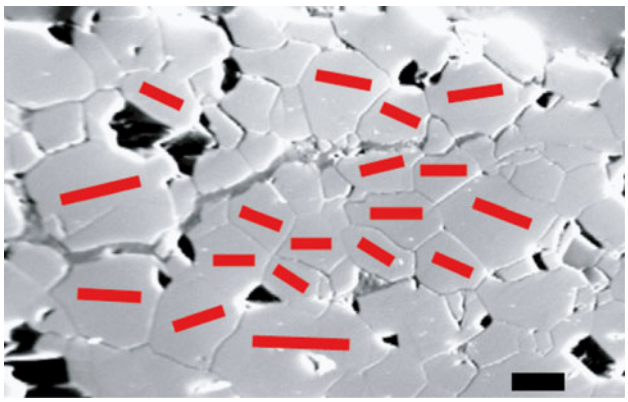

Fig. 7 BSE image showing the relation between grain shape and *c*-axis orientations (*red lines*) of quartz grains in agate annealed at 800°C and 0.5 GPa for 66 h. The *scale* is 10 μm

of foam texture. In the case of quartz, the boundary facets preferentially occupy specific crystallographic orientations, being rhombohedral (Kruhl 2001). Indeed, some of the present grains have boundary facets that are subparallel to rhombohedral (Fig. 7). Because the starting material (agate) of the present experiments has a primary CPO, it is likely that the SPO resulted from the CPO of the agate, demonstrating that quartz grains, and especially their shape, are influenced by crystallographic anisotropy during normal grain growth. It suggests that this effect of crystallographic anisotropy on the normal grain growth of quartz may be important in determining the final microstructure, for instance, in the case of post-deformational grain growth after the development of a quartz CPO.

Acknowledgments We thank T. Masuda, I. Shimizu, M. Kumazawa, Y. Kato, and Y. Watanabe for their help in establishing the Rock-Deformation Experimental Laboratory at Shizuoka University. We also thank Y. Nasuda for assistance during the experiments, T. Hiraga and J. Muto for valuable comments during the study, T. Ubukata, T. Ohuchi and D. Yamazaki for the data analyses, A. Stallard for

improving the English, and an anonymous reviewer for thoughtful comments. This work was supported by grants from the Japan Society for the Promotion of Science (K. Michibayashi) and from the Cooperative Research Programs of the Earthquake Research Institute, University of Tokyo.

References

Atkinson HV (1988) Theories of normal grain growth in pure single phase systems. Acta Metall 36:469–491

Austin NJ, Evans B (2007) Paleowattmeters: a scaling relation for dynamically recrystallized grain size. Geology 35:343–346

Evans B, Renner J, Hirth G (2001) A few remarks on the kinetics of static grain growth in rocks. Int J Earth Sci 90:88–103

Imoto H, Michibayashi K (2010) Grain growth experiments of quartz aggregates in agate under 1 GPa and 800°C. Geoscience Report of Shizuoka University 37:13–19 (in Japanese with English abstract). http://hdl.handle.net/10297/5288

Karato S (2008) Deformation of earth Materials. An introduction to the Rheology of solid earth, Cambridge University Press, Cambridge, pp 463

Katayama I, Hirauchi K, Michibayashi K, Ando J (2009) Trench-parallel anisotropy produced by serpentine deformation in the hydrated mantle wedge. Nature 461:1114–1117

Kruhl JH (2001) Crystallographic control on the development of foam textures in quartz, plagioclase and analogue material. Int J Earth Sci 90:104–117

Masuda T, Fujimura A (1981) Microstructural development of fine-grained quartz aggregates by syntectonic recrystallization. Tectonophysics 72:105–128

Masuda T, Morikawa T, Nakayama T, Suzuki S (1997) Grain-boundary migration of quartz during annealing experiments at high temperatures and pressures, with implications for metamorphic geology. J Metamorph Geol 15:311–322

Michibayashi K, Masuda T (1993) Shearing in granitoids during progressive retrogression: abrupt grain size reduction of quartz at the plastic-brittle transition of feldspar. J Struct Geol 15:1421–1432

Michibayashi K, Tasaka M, Ohara Y, Ishii T, Okamoto A, Fryer P (2007) Variable microstructure of peridotite samples from the southern Mariana Trench: evidence of a complex tectonic evolution. Tectonophysics 444:111–118

Michibayashi K, Oohara Y, Satsukawa T, Ishimaru S, Arai S, Okrugin VM (2009) Rock seismic anisotropy of the low velocity zone beneath the volcanic front in the mantle wedge. Geophys Res Lett 36:L12305. doi:10.1029/2009GL038527

Muramoto M, Michibayashi K, Ando J, Kagi H (2011) Rheological contrast between garnet and clinopyroxene in the mantle wedge: an example from Higashi-akaishi peridotite mass, SW Japan. Phys Earth Planet Interiors 184:14–33

Ohuchi T, Nakamura M (2007) Grain growth in the forsterite-diopside system. Phys Earth Planet Int 160:1–21

Shimizu I, Michibayashi K, Watanabe Y, Masuda T, Kumazawa M (2006) The design and performance of the solid-medium deformation apparatus MK65S: evaluation of the internal friction. Jpn J Struct Geol 49:15–26 (in Japanese with English abstract)

Tullis J, Yund RA (1982) Grain growth kinetics of quartz and calcite aggregates. J Geol 90:301–318

Ueta N, Michibayashi K (2010) Grain growth experiments of quartz aggregates in flint under 1 GPa and 800°C. Geoscience Reports of Shizuoka University 37:21–26 (in Japanese with English abstract). http://hdl.handle.net/10297/5289

Watanabe Y (2007) Microstructural development of quartz aggregate: an experimental study on agate. Master Thesis of Shizuoka University, Shizuoka, pp 26 (in Japanese with English abstract)

Yamazaki D, Inoue T, Okamoto M, Irifune T (2005) Grain growth kinetics of ringwoodite and its implication for rheology of the subducting slab. Earth Planet Sci Lett 236:871–881